

## Auger electron emission from Al induced by keV Ar bombardment: Experiments and Monte Carlo simulations

Oscar Grizzi\* and Raúl A. Baragiola†

*Centro Atómico Bariloche, Comisión Nacional de Energía Atómica, 8400 Bariloche R.N., Argentina*

(Received 28 April 1986)

We have used a Monte Carlo program to study the Al  $L_{2,3}$  Auger electron spectra induced by 1–10-keV Ar ions at 45° incidence. From a comparison of experimental intensities of the main atomic line and the number of excited sputtered recoils we have evaluated the relative role of symmetric and asymmetric exciting collisions. Angular and energy distributions of the excited sputtered atoms were calculated for different  $L_{2,3}$  vacancy lifetimes in the solid, and from these distributions we obtained the energy shifts of the Auger energies. By including the interaction between the metal surface and the excited sputtered atoms we have reproduced the shape of the main atomic line for various values of the projectile energy.

### I. INTRODUCTION

Auger electron spectra of light solids, such as Mg, Al, and Si, induced by heavy-ion bombardment, consist of sharp atomiclike features superimposed on a broad peak. The broad structure is similar to that observed under electron bombardment and is assigned to  $L_{2,3}VV$  Auger transitions from excited target atoms decaying in the bulk, while the sharp atomic lines arise from Auger transitions in excited sputtered atoms decaying outside the solid.<sup>1–6</sup>

At low projectile energies, near the excitation threshold, some previous works<sup>1,2,5–8</sup> confirmed that the inner-shell excitations are produced in symmetric collisions between target atoms (t-t) in the collision cascade. For higher projectile energies, experimental works done in gas-phase atomic collisions<sup>9,10</sup> showed that collisions between the projectile and target atoms (p-t) may produce excitations too. Therefore, it is interesting to study at what energies the p-t contribution begins to be important.

The study of the shape of the atomic lines may also contribute to the understanding of collisional processes. Whaley and Thomas<sup>4</sup> proposed a detailed modeling which accounts for all the Auger peaks of Mg, Al, and Si spectra, where the atomic lines are fitted by Gaussians. Baragiola *et al.*<sup>2</sup> found that the atomic lines broaden towards higher electron energies with increasing projectile energies ( $E_p$ ), and ascribed this broadening<sup>3,4,7,11</sup> to Doppler shift in the Auger energies of the excited sputtered recoils. Contrary to these observations, it was found<sup>12</sup> that, for the same collisional system but different experimental setup, the peak width remains almost constant with  $E_p$ . Recently, Pepper and Aron<sup>13</sup> studied the shape of the main Al atomic line in Ne-Al collisions for various angles of incidence and of the emitted electrons. They found asymmetric spectral structures at particular incidence and observation angles, which could explain the different behaviors observed<sup>2,12</sup> in the atomic lines.

The purpose of this work is to study the p-t and t-t contributions to the excited sputtering yield and the shape of the atomic lines for various values of  $E_p$ . To this end, we

modified a Monte Carlo program to include processes of excitation and decay.

Other calculations,<sup>5,8,14</sup> based on similar computer programs, have been reported. In these works some features of the ion-induced Auger spectra, such as the distributions of the positions of the excitations<sup>8</sup> and of the Auger decays,<sup>5</sup> the Auger intensities versus the angle of incidence of the projectiles<sup>5</sup> and absolute Auger yields<sup>14</sup> were described. A different analytical approach was used by Kudo *et al.*<sup>15</sup> to study the energy degradation of Si  $K$ -shell Auger electrons resulting from  $H^+$  bombardment of a single-crystal silicon target. From the comparison between the measured and calculated Si Auger spectra, they have obtained information about the inelastic mean free path and the mean excitation energy of the Si Auger electrons.

In the following section we describe the experimental setup and the computer program. Thereafter, the simulated atomic yields and ratios of atomic to bulk yields are compared with the experimental results. In Sec. V we calculate the Doppler-shift distributions of the Auger electron energies and the interaction of the excited sputtered recoils with the metal surface. These distributions allow us to reproduce the shape of the main atomic line of Al.

### II. EXPERIMENT

The measurements were performed with ultrahigh-vacuum equipment which was described elsewhere.<sup>2</sup> The sample is a high-purity (>99.999%) aluminum disk, cleaned by sputtering with  $Ar^+$  ions.

The projectiles used in this work were 0.9–10-keV Ar ions, mass analyzed to avoid contamination of the sample. The ion current was in the range  $10^{-9}$ – $10^{-8}$  A, with a spot size of  $\sim 2$  mm of diameter. The incidence angle of the projectiles was 45° with respect to the sample normal.

The electrons ejected during bombardment were energy analyzed with a hemispherical electrostatic energy analyzer, working with a resolution better than 0.2 eV. All the electron energies are referred to the vacuum level;

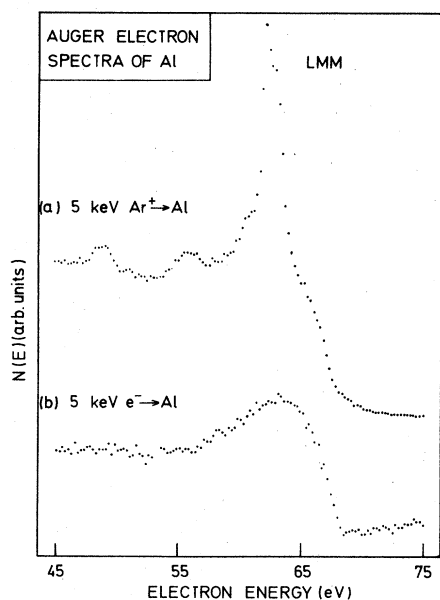


FIG. 1. Energy distributions of electrons ejected from Al by (a) 5-keV Ar ions and (b) 5-keV electrons. In both cases, electron energies are referred to the vacuum level of the target. The spectra were corrected for the energy-dependent transmission function of the analyzer. The channel width was 0.25 eV.

the calibration of the energy scale has been previously described.<sup>2</sup>

In Fig. 1 we show two typical spectra, one, Fig. 1(a), induced by bombardment with 5-keV Ar ions and the other, Fig. 1(b), by 5-keV electron bombardment. In Secs. IV and V we will center our attention on the area and shape of the main atomic line [indicated in Fig. 1(a) as *LMM*], and attempt to separate this atomic line from the bulk contribution by using the electron-induced spectrum of Fig. 1(b).

### III. COMPUTER SIMULATION

We will give here a brief outline of the computer simulation program, which is a modification of that used in a previous study on Be *K*-shell excitation.<sup>16</sup> The program calculates many single-particle trajectories inside the solid. Incident atoms with specified values of initial energy, position, and direction are traced until their energy falls below a cutoff value or until the atoms leave the solid. The particles move in straight-line segments, changing their directions in binary collisions with stationary target atoms placed at the end of each segment. The target is assumed to be amorphous with randomly located atoms and the moving particles have a fixed free-flight path between collisions,  $L = N^{-1/3}$ , where  $N$  is the target-atom density.

Scattering angles are calculated by means of an analytic method<sup>17</sup> based on the Moliere approximation to the Thomas-Fermi interaction potential. The azimuthal scattering angles and the impact parameters are randomly selected. The energy of the moving atoms decreases as a consequence of nuclear and electronic energy losses.<sup>18</sup>

Fast recoils are treated as new projectiles if their kinetic energies are sufficiently high to produce *L*-shell excitation in subsequent target-target (*t-t*) collisions. In each *t-t* collision the program calculates the probability for Al *2p* vacancy production as a function of the distance of closest approach ( $R$ ) in that collision. If  $R$  is lower than a critical value,<sup>2</sup>  $R_c = 0.54 \text{ \AA}$ , one of the two colliding atoms is excited. We assumed equal excitation probabilities for both colliding partners.

Excited recoils are traced until they either decay inside the solid or leave it keeping their state of excitation, decaying later in vacuum. We evaluate the decay probability in a free flight path ( $L$ ) as  $1 - \exp(-t/T_{\text{sol}})$  where  $T_{\text{sol}}$  is the *2p*-hole lifetime in the solid and  $t$  is the time the particle uses to cover the distance  $L$ . The distance traveled by the excited recoil before decaying and the probability for leaving the solid without decaying depends strongly on the value used for the *2p*-hole lifetime.

In Fig. 2 we show the depth distribution of the Al *L*-shell excitations for 2-keV Ar on Al impinging at 45° with respect to the surface normal. The distribution presents an asymmetric shape, and most of the excitations occur between 2 and 16 Å, with a maximum at ~7 Å from the surface. We see that there are excitations at positions deeper than 20 Å. We also show in this figure the distributions of the decay positions for three different lifetimes:  $2 \times 10^{-13}$ ,  $10^{-14}$ , and  $10^{-15}$  sec where the first value corresponds to the calculated lifetime in vacuum,<sup>19</sup> the second is the observed one in solid targets,<sup>20</sup> and the third value is  $\frac{1}{10}$  of the latter. These results are similar to those previously obtained by Andreadis *et al.*<sup>5</sup> The symbols on the vertical axis are proportional to the number of excited recoils ejected from the solid. We see in Fig. 2 that for a lifetime of  $10^{-15}$  sec, the recoils would decay nearly at the same position they were excited, and the probability of ob-

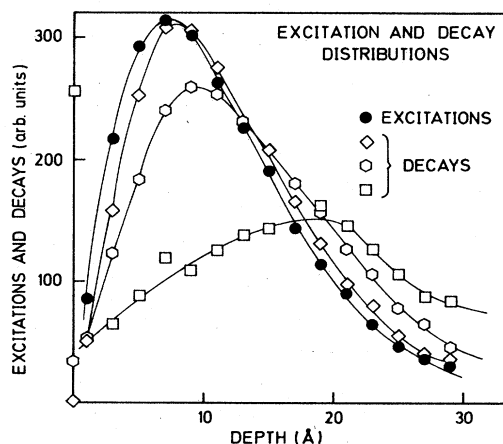


FIG. 2. Distributions of the excitation and decay positions. The closed circles correspond to Al *L*-shell excitations induced by 2-keV Ar ions impinging at 45°. The other distributions correspond to the decay positions for three different *2p*-hole lifetimes in the solid:  $T_{\text{sol}} = 10^{-15}$  sec, ○;  $T_{\text{sol}} = 10^{-14}$  sec, ◇; and  $T_{\text{sol}} = 2 \times 10^{-13}$  sec, □. The symbols on the vertical axis are proportional to the number of excited recoils ejected from the solid.

TABLE I. Simulated and experimental ratios of atomic to bandlike contributions.

$T_{\text{sol}}$ (sec) \backslash $E_p$ (keV)	$10^{-15}$	$10^{-14}$	$2 \times 10^{-13}$	Expt.
2	0.006	0.1	1.4	0.14
10	0.02	0.25	2	0.20

taining excited sputtered recoils would be very low. For  $T_{\text{sol}} = 2 \times 10^{-13}$  sec the recoils would decay far from their excitation position and many of them would escape in excited states.

To go further in the calculations we must choose an appropriate value for the lifetime parameter. An estimation may be derived from the comparison of experimental and simulated ratios of atomic to bulk intensities. Nevertheless, we cannot obtain reliable values of  $T_{\text{sol}}$  due to the uncertainties in the values of the mean free path of Auger electrons in solids<sup>15</sup> and the difficulties in obtaining the experimental bandlike intensity from the Auger electron spectrum. A rough estimate,<sup>5</sup> based on the Auger electron distribution of Powell,<sup>21</sup> yields experimental ratios of atomic to bulk Auger intensities of  $\sim 0.14$  at  $E_p = 2$  keV and  $\sim 0.22$  at 10 keV. Using a mean free path<sup>5</sup> of 4.7 Å for Al Auger electrons we obtained the values shown in Table I for the three values of lifetimes mentioned previously. The best agreement is obtained by using  $T_{\text{sol}} = 10^{-14}$  sec, which is a remarkable result since it is about the  $T_{\text{sol}}$  value one can expect in solids. In the following sections we use this  $T_{\text{sol}}$  to reproduce both the variations of the atomic yields with the projectile energy and the shape of the atomic line.

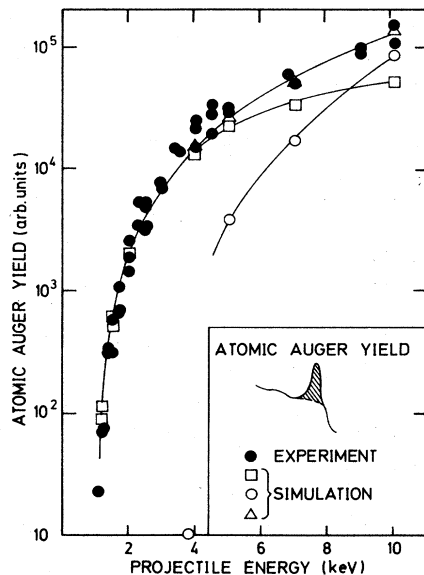


FIG. 3. Experimental yields of the main Auger atomic line of Al and calculated numbers of excited sputtered atoms versus the projectile energy ( $E_p$ ). Shown are calculations of the contributions to the total yield of excited sputtered atoms: t-t contributions,  $\square$ ; p-t contributions,  $\circ$ ; and the sum of them,  $\triangle$ . The results of the simulation were normalized to experiment at  $E_p = 2$  keV.

#### IV. ATOMIC YIELDS

Figure 3 shows the experimental yields of the main atomic-line and the number of excited recoils ejected from the solid versus the projectile energy ( $E_p$ ). At energies below 4 keV, near the excitation threshold, the simulation gives the correct behavior considering that excitation occurs only in target-target (t-t) collisions. This is in agreement with previous works done in the same energy range.<sup>1,2,5-8</sup>

Above 5 keV, the experimental yields increase more rapidly with  $E_p$  than the t-t contribution, indicating as previously suggested<sup>4,9-11,14</sup> that projectile-target collisions may begin to produce significant excitations in this energy region. To evaluate this p-t contribution we need the critical distance to excite the Al  $L$ -shell in an Ar-Al collision. Schneider *et al.*<sup>9,10</sup> observed Si  $L$ -shell excitation in Si-Ar collisions and used a critical distance  $R_c = 0.65$  a.u. for this system. Comparing the correlation diagrams for Si-Ar<sup>9</sup> and Al-Ar<sup>22</sup> systems we obtained  $R_c(\text{Al}) = \sim 0.7$  a.u. In Fig. 3 we present both t-t and p-t contributions to the total yields of excited sputtered atoms. Their sum, normalized to the measured yield at  $E_p = 2$  keV, is found to be in good agreement with experiment.

#### V. ATOMIC LINE SHAPE

The shape of the atomiclike component of the Al Auger spectrum induced by ion bombardment has been the subject of various previous studies.<sup>2,4,12,13</sup> Here we present an analytical estimate of the shape and energy position of the atomic lines based on the calculation of angular and velocity distributions of the excited sputtered recoils. We compare the results of this model with our experimental observations.

The most important factors which determine the shape of the atomic lines are (1) the Doppler shifts of the Auger energies due to the velocity of the excited sputtered atoms with respect to the analyzer, (2) the interaction between the metal surface and the decaying atoms, and (3) the possible overlap of multiple peaks [e.g. the unresolved 0.4-eV splitting<sup>2</sup> of the  $2p_{1/2}$  and  $2p_{3/2}$  initial vacancy states, corresponding<sup>2-4,6</sup> to the  $2p^5 3s^2 3p^2 \rightarrow 2p^6 3s 3p$  transition (main line)]. The natural broadening of the atomic lines and the broadening due to the spectrometer resolution are negligible.

##### A. Doppler shifts

The distributions in Doppler shifts can be obtained from the kinetic energy and angular distributions of the excited sputtered atoms as  $\Delta E = (0.07 \text{ eV}) [E \text{ (eV)}]^{1/2} \cos\theta$ ,

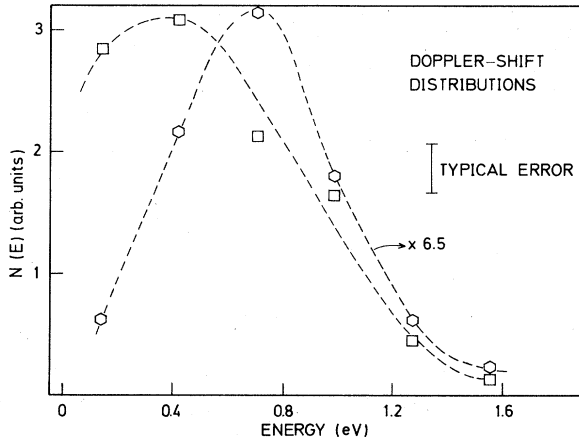


FIG. 4. Doppler-shift distributions of the Auger energies for  $E_p=2$  keV and two values of the  $2p$ -hole lifetime in the solid:  $T_{\text{sol}}=2 \times 10^{-13}$  sec,  $\square$ ; and  $T_{\text{sol}}=10^{-14}$  sec,  $\circ$ . The second distribution was multiplied by a factor of 6.5.

where  $E$  is the kinetic energy of the atom and  $\theta$  the angle between the directions of motion of the atom and of the Auger electron.

Although we have already obtained a value for the  $T_{\text{sol}}$  parameter of  $10^{-14}$  sec in the preceding sections, it is worth studying the effect of varying  $T_{\text{sol}}$  in the computer model. In Fig. 4 we show the distribution in Doppler shifts for a projectile energy of 2 keV and two different vacancy lifetimes  $T_{\text{sol}}=10^{-14}$  sec and  $T_{\text{sol}}=2 \times 10^{-13}$  sec. We see in this figure that the yield of excited sputtered atoms increases considerably with increasing  $T_{\text{sol}}$  and the corresponding Doppler-shift distributions shifts to lower energies. The mean kinetic energy of the excited sputtered atoms decreases from  $\sim 360$  eV for  $T_{\text{sol}}=10^{-14}$  sec to  $\sim 220$  eV for  $T_{\text{sol}}=2 \times 10^{-13}$  sec. A larger  $T_{\text{sol}}$  implies that the excited recoils travel a larger distance before decaying and thus more excited recoils with low kinetic energy may escape, producing the effects shown in Fig. 4.

For projectile energies above 5 keV we must consider two contributions to the Doppler-shift distributions of the excited sputtered recoils: one arising from t-t and another from p-t excitation collisions. The first one is similar to that discussed above for  $E_p=2$  keV (Fig. 5); it is, however, somewhat broader, the maximum is shifted  $\sim 0.4$  eV to higher energies and the mean kinetic energy of the recoils is  $\sim 800$  eV.

The distribution coming from p-t excitation collisions is quite different: it is narrower, with its maximum placed near 0.15 eV and a mean recoil of  $\sim 1100$  eV (see Fig. 5). This means that most of the recoils are ejected at grazing angles, (in a direction perpendicular to that of the observation). Thus the energy of the electrons observed from that part of the recoil flux would have almost no Doppler shift. Nevertheless, these recoils ejected at grazing angles can undergo further deflections by interaction with surface atoms. This effect may alter appreciably the shape of the distributions and it is not taken into account by our program. For such a reason these results must be taken as being only qualitative. We leave for the end of this sec-

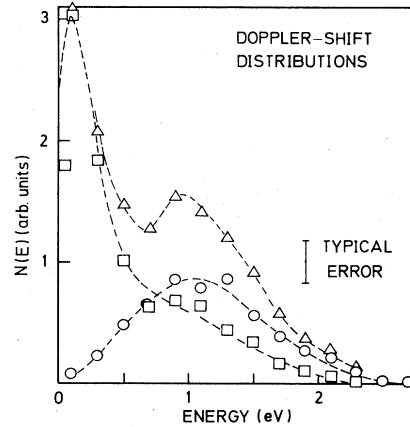


FIG. 5. Doppler-shift distributions of the Auger energies for  $E_p=10$  keV and  $T_{\text{sol}}=10^{-14}$  sec. Contribution from t-t excitation collisions,  $\circ$ ; contribution from p-t excitation collisions,  $\square$ ; and the sum of both contributions,  $\triangle$ .

tion the discussion of the double-peaked distribution resulting from the sum of the t-t and p-t contributions, whose behavior might explain the observations of Pepper and Aron.<sup>13</sup>

## B. Recoil-surface interaction

The shape of the atomic lines is also affected by the interaction between the recoil and the metal surface. To perform an estimate of this interaction we have to know the positions at which the recoils decay. These may be obtained from the angular and velocity distributions provided that the  $LMM$  lifetime of the transition outside the solid ( $T_{\text{vac}}$ ) is known. Unfortunately the lifetimes of neutral atoms have not been measured nor calculated; furthermore, their value may depend on the distance to the solid surface. However, we can guess that the upper limit of  $T_{\text{vac}}$  should be that of the free atom<sup>19</sup> ( $2 \times 10^{-13}$  sec), and the lower limit that of the solid<sup>20</sup> ( $10^{-14}$  sec). We used  $T_{\text{vac}}=10^{-13}$  sec, since this value corresponds approximately to that calculated<sup>19</sup> for the lifetime of the Si atom, in the same final vacancy configuration than the associated<sup>2-4,6</sup> with the main Al atomic line ( $Z+1$  approximation<sup>5</sup>). In Fig. 6 we show the distributions of decay positions, the projectile energy is 2 keV and the lifetime in the solid  $T_{\text{sol}}=10^{-14}$  sec. We can see in this figure that only a small fraction (13%) of the ejected recoil flux decays within the first 3 Å. This allows us to use a simplified model for the recoil-surface (r-s) interaction.

At large projectile energies, those recoils coming from p-t excitation collisions escape from the solid at small angles from the surface, therefore a large fraction of them decay near the surface and our model becomes less accurate.

The energy levels of the recoils evolve as they leave the solid, changing from those of the bulk to those of the free atom; they shift and become narrower. This energy shift is a consequence of the combined action of three potentials: (1) the repulsive potential resulting from the overlap

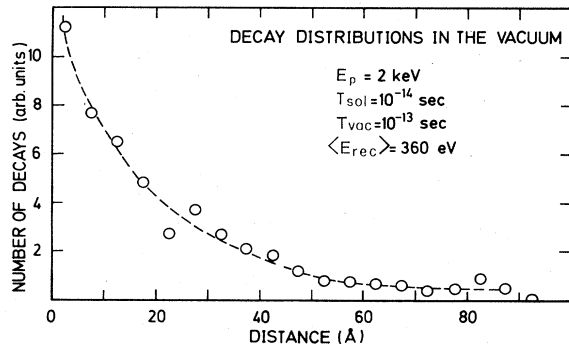


FIG. 6. Distribution of the decay positions of the excited sputtered atoms. The distance is measured from the positive background of the solid surface. The  $2p$ -hole lifetime in the vacuum ( $T_{vac}$ ) was assumed to be independent of the distance to the surface. Note that only a small fraction of the ejected recoil flux decays within the first angstroms.

of the electronic clouds of the particle and of the solid, (2) the image attraction between the ion and the metal, and (3) the van der Waals attraction due to the polarizability of the recoils.

The repulsive force is important at short distances, i.e., around the radius of the maximum charge density of the outermost orbitals. The majority of the excited recoils decay outside this region where this interaction may be neglected.

The image interaction affects the final state of the  $2p^5 3s^2 3p^2 \rightarrow 2p^6 3s 3p$  transition (main atomic line)<sup>2-4,6</sup> and the van der Waals attraction affects both initial and final states.

Using a uniform background model, Lang and Kohn<sup>23</sup> have shown for the image forces that the results of classical elementary electrostatics are valid. Thus for a charge  $q$  situated at  $S$ , the image potential is given by  $V^{im}(S) = -q/4(S - S_0)$ , where  $S_0$  is the center of mass of the electron density distribution. In the case of aluminum  $V^{im}(S) = -(3.6 \text{ eV})/(S - 0.85)$ , where  $S$  is the distance measured from the positive charge in Å.

The van der Waals interaction depends on  $S$  as<sup>24</sup>  $V^W(S) = -C/(S - S_1)^3$ , where  $C$  is a constant determined by the polarizability of the moving particle and  $S_1$  the distance of a reference plane from the metal surface. Approximated expressions for these parameters are<sup>25</sup>

$$C = \frac{g_0 \alpha_0}{8} \frac{E_A E_S}{E_A + E_S}$$

and

$$S_1 = \frac{1}{2} \frac{E_A + 2E_S}{E_A + E_S} S_0,$$

where  $\alpha_0$  is the static atomic polarizability,<sup>26</sup>  $E_A$  an energy characteristic of the atom which can be taken<sup>25</sup> equal to the ionization energy,  $E_S$  a characteristic energy of the solid which may be approximated by the energy of a surface plasmon, and  $g_0$  a quantity which depends only on

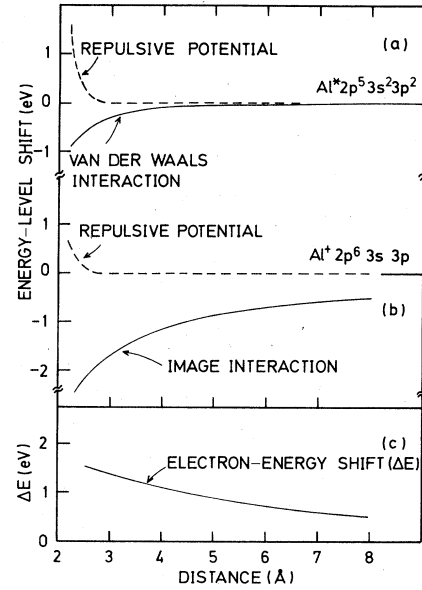


FIG. 7. Diagram of the energy-level shifts due to the recoil-surface interaction corresponding to (a) initial  $\text{Al}^* 2p^5 3s^2 3p^2$  and (b) final  $\text{Al}^+ 2p^6 3s 3p$  states of the main Auger transition in vacuum.<sup>2-4,6</sup> (c) Effect of these energy shifts on the energy of the Auger electrons.

the solid. We evaluated  $g_0$  fitting known values of  $C$ . With these approximations the van der Waals interaction between the excited neutral atom and the metal results  $V^W(S) = -(4 \text{ eV})/(S - 0.6)^3$ , which is much lower than the image interaction, amounting to 17% at  $S = 3 \text{ Å}$  and 1% at  $S = 10 \text{ Å}$ . The van der Waals interaction between the ion and the metal is even lower and can therefore be neglected.

In Fig. 7 we show a diagram of the shifts of the energy levels of the moving particles due to the  $r$ - $s$  interaction, and the effect on the energy of the Auger electrons. The energy shift is larger for those electrons coming from recoils with a small velocity along the direction of the surface normal (recoils decaying near the surface). This behavior is just the opposite to that caused by the Doppler effect.

In Fig. 8(a) we show the energy shift distributions due to the Doppler effect and the interaction of the recoils with the surface. The parameters used are projectile energy  $E_p = 2 \text{ keV}$ ,  $T_{sol} = 10^{-14} \text{ sec}$ , and  $T_{vac} = 10^{-13} \text{ sec}$ . The main effect of the  $r$ - $s$  interaction is to produce an additional shift of  $\sim 0.4 \text{ eV}$  to higher energies in the atomic lines. If the excited recoils decay nearer to the surface (recoils coming from  $p$ - $t$  excitation collisions at greater projectile energies) the energy shift distributions are more affected in their shape. The same occurs if we consider larger vacancy lifetimes in the solid, for example  $T_{sol} = 2 \times 10^{-13} \text{ sec}$  [Fig. 8(b)]. As said before, for larger  $T_{sol}$ , a greater quantity of slow recoils may escape keeping their state of excitation, therefore more recoils will decay near the surface with small Doppler shifts and large shifts due to  $r$ - $s$  interaction. The total effect is a narrower distribution shifted to higher energies.

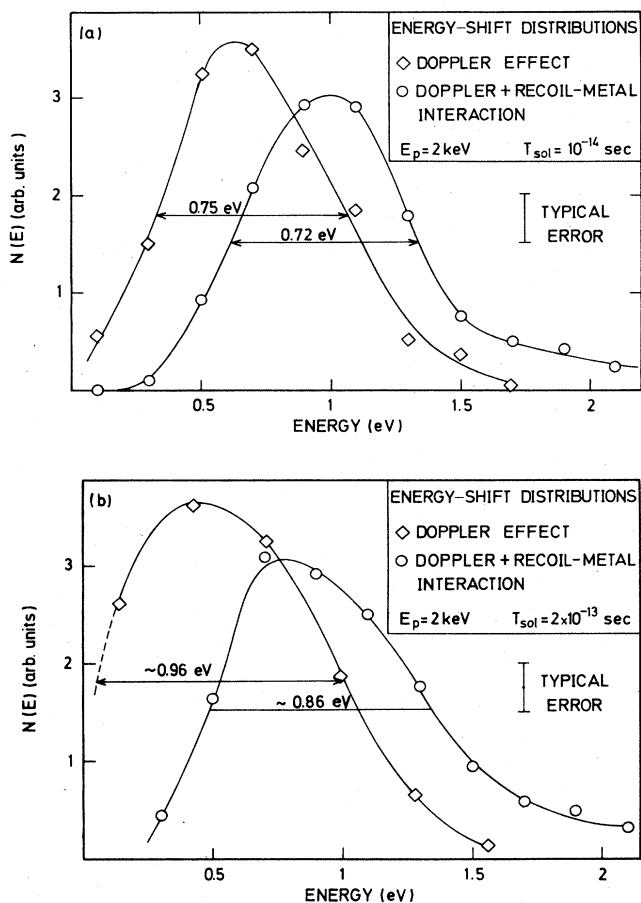


FIG. 8. Energy shift distributions of the Auger electrons due to Doppler effect and the interaction of the excited sputtered recoils with the surface. The parameters used are  $E_p = 2$  keV,  $T_{vac} = 10^{-13}$  sec, (a)  $T_{sol} = 10^{-14}$  sec, and (b)  $T_{sol} = 2 \times 10^{-13}$  sec.

The energy levels of an atom moving near a surface not only shift but also become broader with increasing overlap of the electronic clouds. This broadening ( $\Delta$ ) has an exponential dependence<sup>27</sup> with the distance to the surface  $\Delta = \Delta_0 \exp(-\gamma S)$ . Typical values<sup>27,28</sup> for these parameters produce small effects on the shape of the calculated distributions.

### C. Comparison with experiment

To reproduce the shape of the atomic line we assumed a source of 61.7-eV electrons corresponding<sup>4</sup> to free transitions (vertical arrow in Figs. 9 and 10). This  $\delta$ -like distribution of electrons becomes shifted and broadened by (1) Doppler effect, (2) recoil-surface interaction, and (3) splitting of the initial vacancy state. The base lines for the simulated peaks were obtained comparing the ion and the electron-induced spectra (Fig. 1), normalized at 66 eV.

In Fig. 9 we compare the shape of the main line obtained by bombarding the Al sample with 2-keV Ar ions with the corresponding results of the simulation, normal-

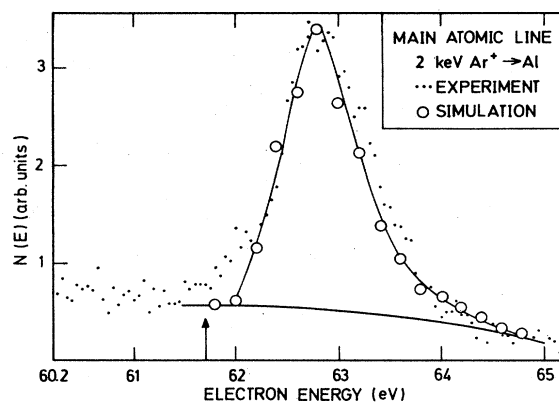


FIG. 9. Comparison of the experimental and simulated shapes of the main Auger atomic line of Al bombarded with 2-keV Ar ions. The simulation was normalized to experiment at 62.8 eV and the base line for the simulated peak was obtained comparing the ion and the electron induced spectra. The vertical arrow at 61.7 eV represents the source of electrons corresponding to free transitions. This  $\delta$ -like distributions of electrons results shifted and broadened, as shown by the circles, by Doppler effect, recoil-surface interaction, and splitting of the initial vacancy state.

ized at 62.8 eV. The agreement obtained in the shape and in the position is quite encouraging, suggesting that the approximations and parameters used in the model are reasonably good.

In Fig. 10 we compare the electron distributions for a projectile energy of 10 keV (the highest energy for which we measured spectra). Here the agreement is also good. The structure appearing at 62 eV in the calculated atomic peak, when only the distributions in Doppler shifts were taken into account, is similar to that observed in the spectra of Pepper and Aron<sup>13</sup> and in our spectra. We have observed the same structures in experiments with Mg and Si bombarded with different projectiles. When the recoil-

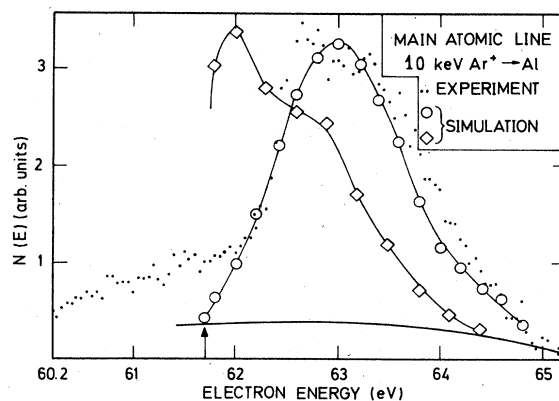


FIG. 10. Comparison of the experimental and simulated shapes of the Auger atomic line of Al for  $E_p = 10$  keV. Energy shift distributions due to Doppler effect and splitting of the initial vacancy state,  $\diamond$ ; and the same distribution including the Doppler effect, splitting, and recoil-surface interaction,  $\circ$ .

surface interaction is included this structure disappears, but we must remember that it comes from the recoils excited in p-t collisions and that our model is not accurate for this part of the ejected flux.

The shape of the main atomic line for other projectile energies, 3, 4, 5, and 7 keV (not shown in this work), were reproduced with similar results.

## VI. CONCLUSIONS

The comparison of the results of the Monte Carlo simulation with the experimental Al  $L_{2,3}$ MM Auger electron spectra induced by Ar bombardment have led to the following conclusions. (1) For projectile energies below 5 keV, near the excitation threshold, the excitations are produced mainly in symmetric collisions between target atoms of the collision cascade. (2) The asymmetric collisions, between a projectile and a target atom, begin to produce significative excitations in the energy range 5–10 keV. At these projectile energies the angular distributions of the sputtered atoms excited in t-t collisions are different from those excited in p-t collisions. For incidence angles of the projectiles of 45°, most of the sputtered atoms excited in p-t collisions are ejected at angles close to the surface, where the intereaction of this part of the sputtered flux with the metal surface is strong. (3) The

Doppler shifts in the Auger electron energies of the excited sputtered atoms are the main cause of broadening of the atomic lines. These energy shifts were calculated from the energy and angular distributions of the sputtered atoms. Including the interaction of the ejected atoms with the metal surface, the shape of the atomic lines were reproduced with good agreement with experiments.

This and other works<sup>5,8,14</sup> show that many features of the ion-induced Auger electron spectra of solids may be studied by means of Monte Carlo programs. Particularly, as was suggested previously,<sup>13</sup> the study of the variations of the atomic line shape with the incidence angle of the projectiles and the observation angle of the ejected electrons may give information about the collisional models. Further work along this line is being done in our laboratory.

## ACKNOWLEDGMENTS

We would like to thank the following people for useful discussions: V. H. Ponce, E. V. Alonso, M. M. Jakas, G. E. Zampieri, and M. Abbate. This work was partially supported by the Secretaría de Ciencia y Tecnología and the Consejo Nacional de Investigaciones Científicas y Técnicas (Argentina).

\*Also at Universidad Nacional del Comahue, Centro Regional Bariloche, 8400 S.C. de Bariloche, R.N., Argentina.

†Present address: ALTEC Sociedad del Estado, Casilla de Correo 112, 8400 S.C. de Bariloche, R. N., Argentina.

<sup>1</sup>R. A. Baragiola, in *Inelastic Particle-Surface Collisions*, Vol. 17 of *Springer Series in Chemical Physics*, edited by E. Taglauer and W. Heiland (Springer, Berlin, 1981), p. 38.

<sup>2</sup>R. A. Baragiola, E. V. Alonso, and H. J. L. Raiti, *Phys. Rev. A* **25**, 1969 (1982).

<sup>3</sup>W. A. Metz, K. O. Legg, and E. W. Thomas, *J. Appl. Phys.* **51**, 2888 (1980).

<sup>4</sup>R. Whaley and E. W. Thomas, *J. Appl. Phys.* **56**, 1505 (1984).

<sup>5</sup>T. D. Andreadis, J. Fine, and J. A. D. Matthew, *Nucl. Instrum. Methods* **209/210**, 495 (1983).

<sup>6</sup>J. A. D. Matthew, *Phys. Scr.* **T6**, 79 (1983).

<sup>7</sup>K. Wittmaack, *Surf. Sci.* **85**, 69 (1979).

<sup>8</sup>J. J. Vrakking and A. Kroes, *Surf. Sci.* **84**, 153 (1979).

<sup>9</sup>D. Schneider, G. Nolte, U. Wille, and N. Stolterfoht, *Phys. Rev. A* **28**, 161 (1983).

<sup>10</sup>D. Schneider, U. Wille, N. Stolterfoht, and G. Nolte, *Phys. Rev. A* **33**, 2099 (1986).

<sup>11</sup>C. Benazeth, N. Benazeth, and L. Viel, *Surf. Sci.* **78**, 625 (1978).

<sup>12</sup>K. Saiki and S. Tanaka, *Nucl. Instrum. Methods Phys. Res. B* **2**, 512 (1984).

<sup>13</sup>S. V. Pepper and P. R. Aron, *Surf. Sci.* (to be published).

<sup>14</sup>C. Benazeth and N. Benazeth, *Surf. Sci. Lett.* **151**, L137 (1985).

<sup>15</sup>H. Kudo, D. Schneider, E. P. Kanter, P. W. Arcuni, and E. A. Johnson, *Phys. Rev. B* **30**, 4899 (1984).

<sup>16</sup>O. Grizzi and R. A. Baragiola, *Phys. Rev. A* **30**, 2297 (1984).

<sup>17</sup>J. P. Biersack and L. G. Haggmark, *Nucl. Instrum. Methods* **174**, 257 (1980); J. P. Biersack and W. Eckstein, *Appl. Phys. A* **34**, 73 (1984).

<sup>18</sup>J. Lindhard and M. Scharf, *Phys. Rev.* **124**, 128 (1961).

<sup>19</sup>D. L. Walters and C. P. Bhalla, *Phys. Rev. A* **4**, 2164 (1971).

<sup>20</sup>M. Citrin, G. K. Wertheim, and M. Schluter, *Phys. Rev. B* **20**, 3067 (1979).

<sup>21</sup>C. J. Powell, *Phys. Rev. Lett.* **30**, 1179 (1973).

<sup>22</sup>F. P. Larkins, *Proceedings of the International Conference on Inner Shell Ionization Phenomena and Future Applications*, Oak Ridge, 1972, edited by R. W. Fink, S. T. Manson, J. M. Palms, and P. Venugopala Rao (unpublished).

<sup>23</sup>N. D. Lang and W. Kohn, *Phys. Rev. B* **7**, 3541 (1973).

<sup>24</sup>E. Zaremba and W. Kohn, *Phys. Rev. B* **13**, 2270 (1976).

<sup>25</sup>G. Vidali and M. W. Cole, *Surf. Sci.* **110**, 10 (1981).

<sup>26</sup>S. Fraga, J. Karwowski, and K. M. S. Saxena, *At. Data Nucl. Data Tables* **12**, 467 (1973).

<sup>27</sup>N. D. Lang, *Phys. Rev. B* **27**, 2019 (1983).

<sup>28</sup>N. D. Lang and A. R. Williams, *Phys. Rev. B* **18**, 616 (1978).